Soil geochemistry of hydrogen and other gases along the San Andreas Fault

Yashee Mathur
Department of Energy Science and Engineering
Stanford University
yashee@stanford.edu

Victor Awosiji
Depart of Earth and Planetary Sciences
Stanford University
vawosiji@stanford.edu

Tapan Mukerji
Department of Energy Science and Engineering
Stanford University
mukerji@stanford.edu

Allegra Hosford Scheirer
Depart of Earth and Planetary Sciences
Stanford University
allegras@stanford.edu

Kenneth E. Peters
Depart of Earth and Planetary Sciences
Stanford University
kepeters@stanford.edu

Version: July 23rd, 2023

Abstract

Natural hydrogen has generated great interest as a potential clean and renewable energy source. To understand the occurrence of natural hydrogen, 103 1-m deep soil gas samples were acquired near the San Andreas Fault at Jasper Ridge and Portola Valley, California, USA. The gas samples were analyzed for hydrogen, helium, carbon dioxide, light hydrocarbons, and fixed gas concentrations. Statistical data analysis was carried out to group samples, reveal their spatial distribution, and understand possible sources of the gases.

High concentrations of hydrogen up to 20.3 ppmv and 17.3 ppmv occur in Jasper Ridge and Portola Valley, respectively, ~ 30-35 times greater than the atmospheric concentration. Most samples with high hydrogen concentrations fall on or near faults, suggesting an origin by serpentinization or geomechanical activation of catalytic sites in minerals, although a deep-seated primordial origin cannot be excluded. Elevated concentrations of carbon dioxide resulted from aerobic microbial degradation of organic matter and elevated concentrations of light hydrocarbons likely resulted from thermal cracking of organic matter.

1. Introduction

The rising climate crisis has stirred interest in hydrogen as an alternative energy source. Global demand for hydrogen increased multifold from 18.2 Mt in 1975 to 94 Mt in 2021 and is expected to rise to 530 Mt by 2050 (IEA, 2021). More than 95% of hydrogen today is produced through steam methane reformation (SMR) or electrolysis. Renewable processes to produce hydrogen include photo-fermentation (Redwood et al., 2012), biomass gasification (Han et al., 2017), water-shift reactions in syngas fermentation (Gunes et al., 2021), or the activity of hydrogen-producing bacteria or microalgae (Oey et al., 2016). None of these processes have achieved price parity with natural gas, and thus, manufactured hydrogen is still an expensive fuel. The fortuitous discovery of 98% pure hydrogen in the Bougou-1 well in Taoudeni Basin, Mali, Africa (Prinzhofer et al., 2018) has opened frontiers for the production and commercialization of natural hydrogen as an alternative fuel. Other hydrogen discoveries are in oil and gas exploration wells in Kansas, USA (Coveney et al., 1987), a mineral deposit mine in the Kola Peninsula (Nivin et al., 2016), hot springs in the eastern coastal area of China (Hao et al., 2020), fluid seepages in New Caledonia

(Deville and Prinzhofer, 2016), oil and gas wells in western Australia (Boreham et al., 2021), mantle mafic rocks in Oman (Neal and Stagner, 1983), and others (see Zgonnik, 2020 for a full set of references).

The primary source of natural hydrogen has been argued to be primordial (Larin, 1993). Others claim that the Earth's interior was originally hydrogen-rich (Shcherbakov and Kozlova, 1986; Toulhoat and Zgonnik, 2022) or that there are significant H_2 concentrations in the core (Isaev et al., 2007). Serpentinization of iron-rich rocks may be a major secondary source of natural hydrogen (Gaucher, 2020; Boreham et al., 2021), and multiple occurrences of hydrogen have been documented near faults where they have also been used for earthquake prediction (Wakita et al., 1980; Ware et al., 1984; Satake et al., 1984; Sato et al., 1984 and 1986, Arai et al., 2008; Fong-liang and Gui-ru (1981); Sugisaki et al., 1983; Rogozhin et al., 2010; Shirokov et al., 2015; Jones and Pirkle, 1981). Wakita et al. (1980) reported up to 3% hydrogen by volume along the Yamasaki fault in southwestern Japan, and Sugisaki et al. (1983) reported up to 9.36% hydrogen along other active faults in Japan. Continuous monitoring of hydrogen was carried out along the San Andreas and Calaveras faults from 1980–84 using a fuel cell sensor and a network of telemetered stations (Sato et al., 1984, 1986). The sensor in their studies only measured H_2, SO_2, and H_2S gases and could have an uncertainty range of up to 25% due to noise and intermittent instrument issues. The hydrogen was hypothesized to originate from chemical reactions between groundwater and fresh surfaces of basement rocks exposed by fault movements (Sato et al., 1984, 1986, Sugisaki et al., 1983; Wakita et al., 1980). Wiersberg and Erzinger (2008) presented multiple hypotheses for the occurrence of up to 10% hydrogen in the SAFOD (San Andreas Fault Observatory at Depth) well and postulated that hydrogen formation took place by the interaction of water with fresh mineral surfaces generated by tectonic activities. Similar interpretations about the generation of high hydrogen concentrations have also been made by Arai et al. (2008) in the Nojima Fault Zone, Japan. Soil gas sampling in Burro Mountain, California near exposures of iron-rich dunnite registered up to 70% hydrogen, which was attributed to the oxidation of ferrous hydroxide (Ware et al., 1984).

Because serpentinization of ultrabasic rocks is one of the most promising sources of natural hydrogen, we chose the Jasper Ridge Biological Preserve (JRBP) and Portola Valley areas as our sampling sites. Additionally, these sites were logistically convenient. At JRBP, serpentinite, deep-

seated ultrabasic rocks, and alluvium deposits occur along Quaternary thrust faults and the San Andreas fault. Portola Valley presents a unique opportunity for the study of mechanoradical hydrogen (Kita et al., 1982) generated by faults because of the presence of the 1906 rupture of the San Andreas fault, undifferentiated Quaternary faults (1.6 m.y.), and late Quaternary faults (<15,000 yr). Geochemical soil gas sampling and related data analysis could be an exploration tool for finding natural hydrogen. We present here the results of extensive sampling, measurement, and analysis of hydrogen, helium, carbon dioxide, light hydrocarbons, and fixed gases, followed by multivariate statistical analysis and spatial correlation. Based on our analysis, we provide hypotheses on the origins of hydrogen and other gases.

2. Sampling sites, materials, and methods

Geology

Jasper Ridge Biological Preserve in the foothills of the Santa Cruz Mountains formed through a complex history of tectonic activity and erosion. The rocks at Jasper Ridge have been extensively faulted, with several active faults running through the preserve that capture the history of continental growth through subduction and accretion for about 150 Ma (Coleman, 2004). The most prominent of these is the San Andreas Fault, which runs along the western edge of the preserve (Figure 1). The geology consists of greenstone, blueschist, chert, sandstone, and serpentinite formed in diverse geological settings (Coleman, 2004 and references therein). Our sampling strategy included samples across all major faults in the region. The sampling points were taken along a transect that cut through various geologic formations with a maximum sampling spacing of 200 m.

Portola Valley is a town in San Mateo County, California, situated in the foothills of the Santa Cruz Mountains. Tectonic activity in the region results from interaction between the Pacific Plate and the North American Plate, which meet at the San Andreas Fault, located just west of Portola Valley. The San Andreas Fault is a transform boundary that is responsible for most of the earthquakes in the region. In addition to the San Andreas Fault, several other faults run through the region, including the San Gregorio Fault and the Pilarcitos Fault (Sloan, 2006). The lithologies comprise graywacke sandstone, greenstone, chert, serpentinite, and the Franciscan complex.

Sampling in Portola Valley was carried out along the faults as well as away from the faults, with greater sampling density in the northern region.

Sampling procedure

A total of 103 gas samples were acquired from Jasper Ridge and Portola Valley (Figure 1). Forty-two samples were from Jasper Ridge and sixty-one samples were from Portola Valley. Four samples from Jasper Ridge and six samples from Portola Valley were repeated in time sequences at specific locations. The time sequence measurements were performed to understand the effects of sediment agitation during and after collection. Splits of four sets of samples were analyzed in duplicate to establish repeatability.

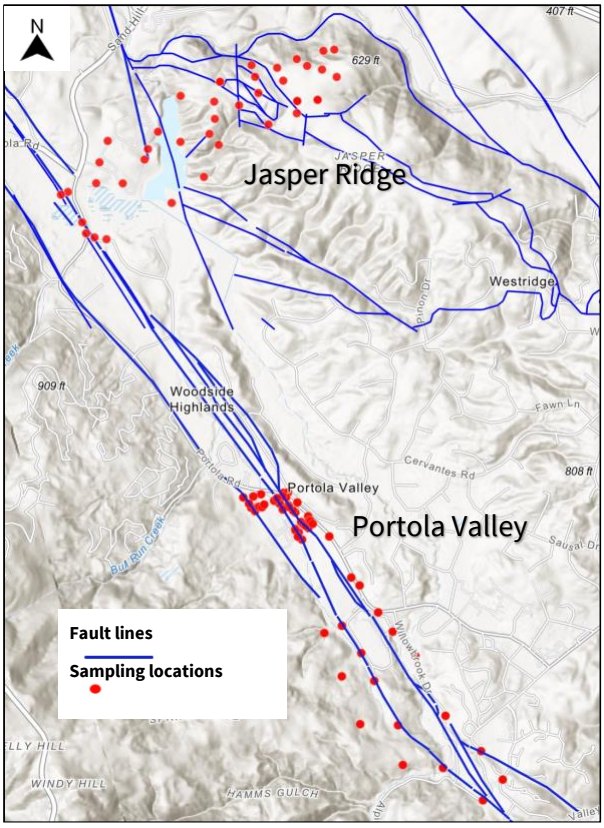

Figure 1: Sampling locations and fault lines at Jasper Ridge (Jasper Ridge Biological Preserve Agency, 2017) and Portola Valley

We used a soil gas probe with a sliding hammer to take soil samples at 1-m depth. Before each day of sampling, we changed the septum, and a leak test was performed through the gas inlet and outlet located 1-m apart on the probe. This ensured that there was no soil or mud blocking the

sampling hole in the probe. Corrective measures were taken whenever there was a leak. To acquire the sample, the probe was pounded into the ground by striking the movable part of the sliding hammer firmly in the downward direction. This was done until the desired 1-m depth was achieved. To flush the previous sample, 4 cc of soil gas was withdrawn through the septum using a syringe and discarded, which is four times the internal volume of the probe. Then we collected 20 cc of soil gas using a syringe, which was immediately evacuated into a clear sample vial and the location was noted using GPS coordinates. The sample vial was labeled and sent for analysis.

Analysis of gases

The gas samples were analyzed for concentrations of hydrogen, helium, carbon dioxide, light hydrocarbons (methane, ethane, propane, *i*-butane, *and n*-butane), and fixed gases (oxygen and nitrogen). The C_1–C_4 hydrocarbons were measured using a gas chromatograph (GC) with a flame ionization detector (FID). The carrier gas for this analysis was helium and air and hydrogen were used to run the flame. For fixed gas analysis, a GC was used with a thermal conductivity detector (TCD) and an FID in series. The carrier gas was argon and the same air and hydrogen were used for the FID. Hydrogen was analyzed using a GC with a reducing gas detector (RGD) and nitrogen as a carrier gas. All gases listed above were of ultra-high purity. The gas chromatographs were equipped with a 1.0-mL sample loop, so roughly 3.0 mL of sample gas was used each time, and the sample loop was completely flushed multiple times to remove ambient air before analysis. This ensures the same amount of sample gas for each analysis.

The helium gas analysis was done using a mass spectrometer with the magnet tuned so that the detector only saw helium-4. The mass spectrometer was calibrated before analysis. The mass spectrometer has a 0.5 mL sample loop, so 1.5 mL of sample or standard gas completely flushes ambient air and consistent amounts of gas were used for each analysis.

Data analysis workflow

We performed multivariate statistical analysis on the gas concentration dataset. We calculated the basic statistics of the dataset to understand variability, followed by gridding and contouring to map the local and regional behavior of different gases. Different clusters of the dataset were established to understand the similarity and relationship between samples using hierarchical cluster analysis (HCA) by employing Euclidean distance metrics. We then performed principal component

analysis (PCA) and visualized the samples in principal component space to further understand the groups of samples. Details of HCA and PCA can be found in standard multivariate statistics books e.g., Hastie et al., 2001. A single sample in our dataset comprises mixtures of multiple gases. Therefore, we performed alternating least squares (ALS) regression to determine the number of probable sources of gas and their proportions in the dataset. Alternating least squares regression (ALS) is a powerful method to deconvolute mixtures in chemistry (Jalalvand and Goicoechea, 2017), geochemistry (Murray and Peters, 2021), and spectroscopy (Lyndgaard et al., 2013) to estimate the contributions of individual components or gases in a sample.

3. Results

We observed elevated concentrations of hydrogen in both study areas with maxima at 20.32 ppmv in JRBP and 17.31 ppmv in Portola Valley. In the JRBP, two distinct regions of high hydrogen contours overlie faults, with the third region very close to a fault (Figure 2a). Exposures of serpentinites occur in this region.

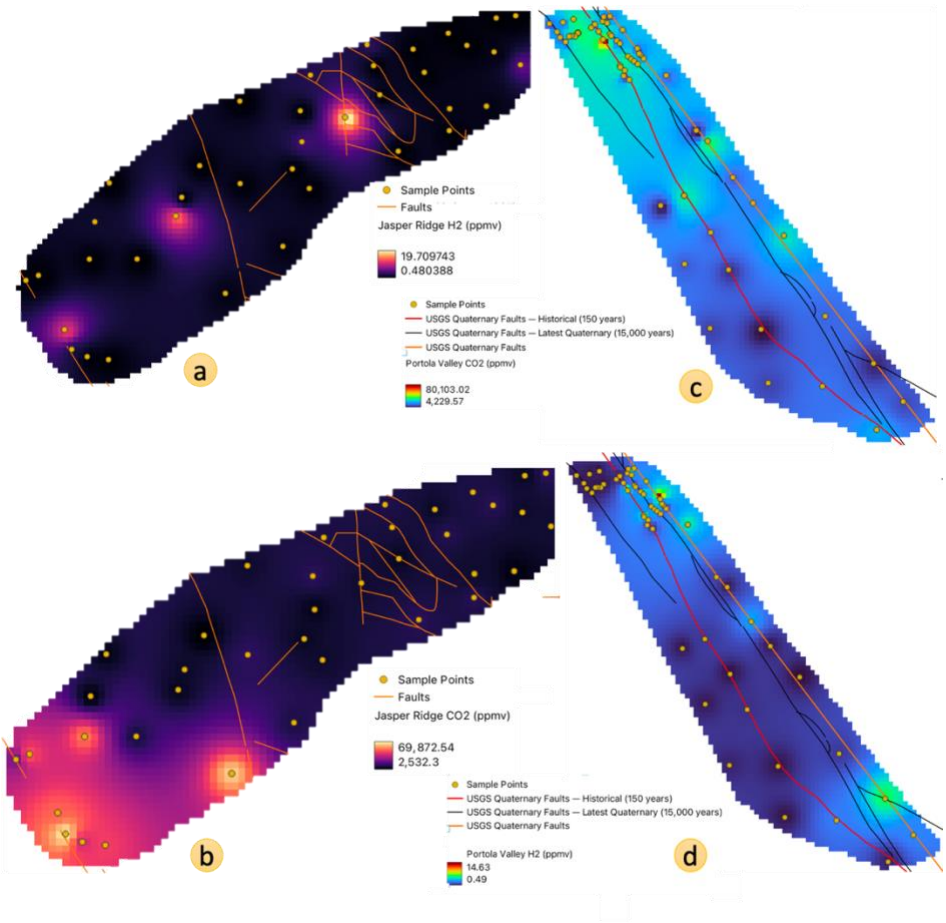

Figure 2: Concentration of a) hydrogen and b) carbon dioxide in Jasper Ridge; concentration of c) hydrogen and d) carbon dioxide in Portola Valley. Jasper Ridge faults retrieved from Jasper Ridge Biological Preserve Agency (2017).

The concentration of helium was uniform, with an average of 5.45 ppmv, which is consistent with the observations of Wakita et al. (1980) in the vicinity of the San Andreas Fault. The concentrations of oxygen and nitrogen were similar to atmospheric concentrations and no carbon monoxide was observed in the gas samples, potentially due to its unstable nature. Anomalous concentrations of carbon dioxide occur in both regions, up to 70,019 ppmv in the southwest part of JRBP (Figure 2b) and up to 90,945 ppmv in the northern part of Portola Valley (Figure 2d).

Time sequence and repeatability analyses

Soil gas hydrogen concentration has been observed to show diurnal changes (Prinzhofer, et al., 2019; Sato et al., 1986). To assess the diurnal variations, we took samples at times 0, 6 hours, and 26 hours at sample locations 1 named 1, 1B, and 1C. Similarly, time sequence samples were taken at location 3 with a gap of 10 minutes and at location 24 after 2 hours. All samples were normalized to the concentration at time t = 0. The concentration of gases first increases and then equilibrates

(Figure 3 left). This appears to be caused by agitation of the soil during initial sampling followed by re-equilibrium over a period of ~24 hours. In addition, lab repeatability was carried out for four samples 3, 3B, 24, and 24B where the concentration of all gases was measured twice on identical splits of the same sample. The standard deviation for methane concentration in these four duplicate samples was 2.52%, 4.14%, 1.42%, and 10.92% showing excellent lab repeatability. In Portola Valley, we conducted time sequence measurements at location 15 at times 0, 10 minutes, 2 hours, 6 hours, 24 hours, and 26 hours. In Figure 3 right the concentration of methane increases for two hours and then drops to near its initial concentration at about five hours.

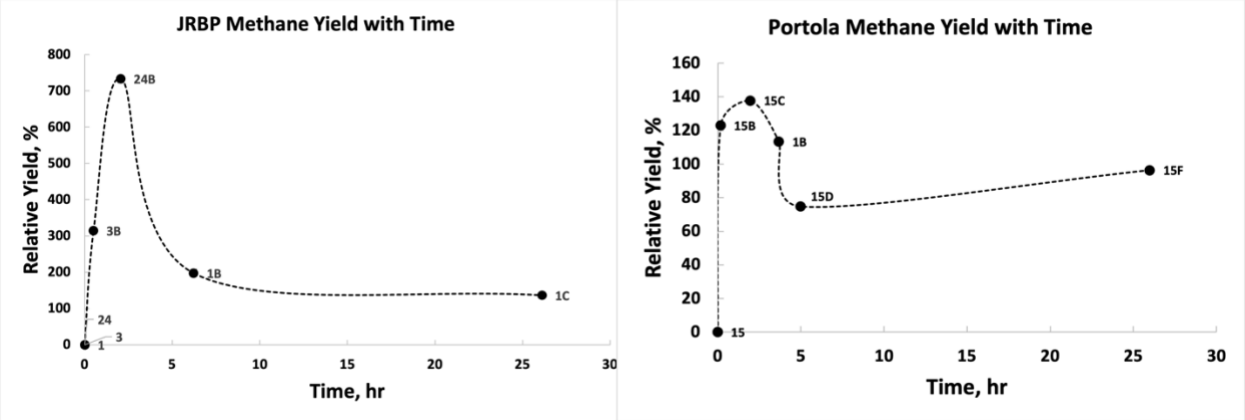

Figure 3: Relative yield of methane vs. time for Jasper Ridge and Portola Valley time sequence samples

3.1. Jasper Ridge Biological Preserve (JRBP)

Data analysis

From the concentrations of gases that were analyzed, we used seven independent variables: hydrogen, carbon dioxide, methane, ethane, propane, *i*-butane, and *n*-butane to carry out further analysis, excluding the repeat samples. We established five clusters in the Jasper Ridge data using HCA, as highlighted in the dendrogram (Figure 4). Principal component analysis (PCA) captures 90.2% of the variance in the dataset using three principal components. We used principal component plots to understand the differences between multiple clusters (Figure 5).

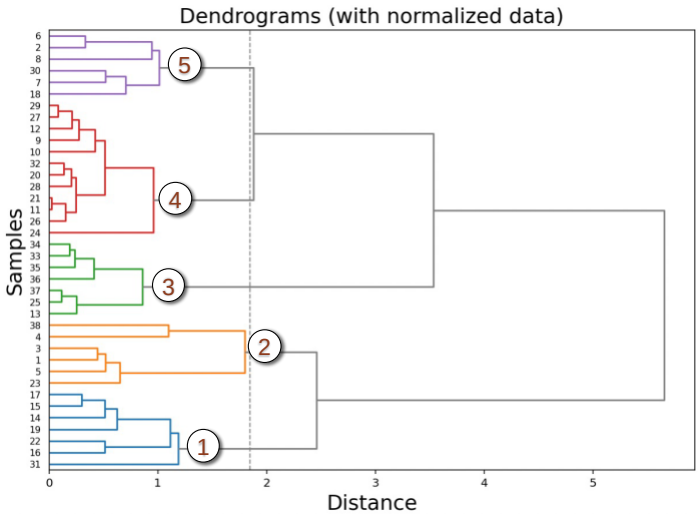

Figure 4: Dendrogram of hierarchical cluster analysis based on Euclidean distance for Jasper Ridge dataset.

In the 1st principal component (PC) vs. 2nd PC plot (Figure 5 left), the third cluster (green) is rich in CO_2, the first and second clusters are rich in light hydrocarbons, and the other clusters show the background gas concentrations. Certain samples from the first cluster also exhibit high H_2 along with high light hydrocarbon concentrations. Similar observations can be made on the 2nd PC vs. 3rd PC plot, except for more separation in the first cluster. To understand the behavior of the clusters and the odd samples, we plotted the elevation of each sample in the clusters (Figure 6). The third cluster has the lowest elevation and highest CO_2 concentrations and lies in the southwest region of Jasper Ridge, with an average elevation of 350 feet. This cluster was in a marshy region with significant vegetation.

Sample 38 also lies in this low-lying region and has high concentrations both of H_2 and CO_2 (Figure 5). It was the closest sample to a nearby water body. Samples 16 and 22 show high H_2 concentrations and overlie a fault.

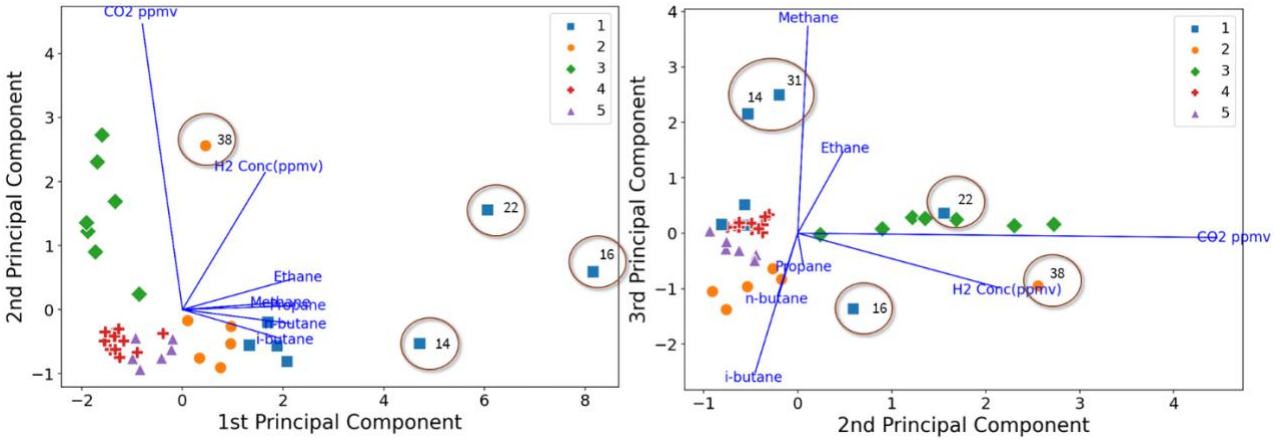

Figure 5: Jasper Ridge: Principal component plots show different clusters identified through HCA, with anomalous samples highlighted. The lines are the loadings, highlighting the correlation of the clusters with the specific gas concentrations.

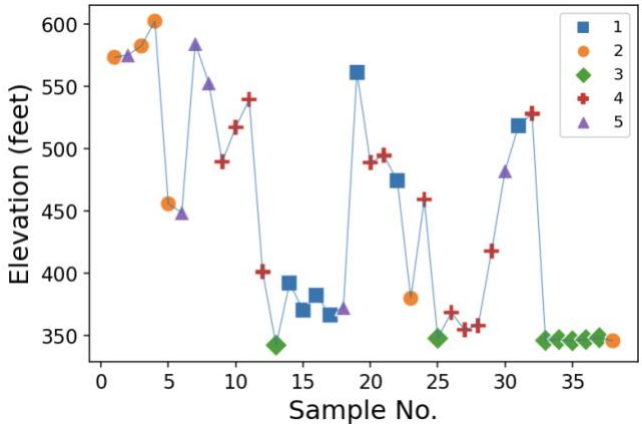

Figure 6: Elevation vs. sample numbers in JRBP

Based on ALS, three endmember sources of gases exist in JRBP. Figure 7 shows linear mixing between the CO_2 endmember (Cluster-3) and the light hydrocarbon endmember (Cluster-1 and 2). The samples that plot away from the linear mixing line (4, 14, 16, 22, 24, 31, 38) are high in hydrogen concentration, indicating a separate endmember. The hydrogen concentration of these samples ranks in the top 25th percentile of all samples measured at Jasper Ridge.

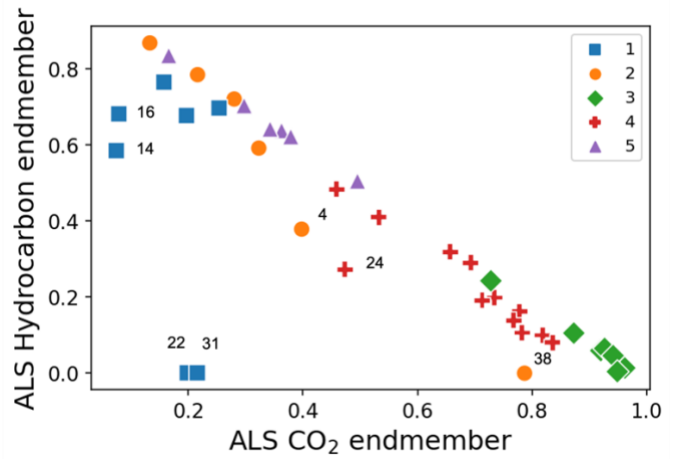

Figure 7: Component 1 vs. component 2 generated using alternating least squares regression.

3.2. Portola Valley

Data analysis

A similar data analysis approach as described earlier established six clusters using seven independent variables in Portola Valley, as shown in the dendrogram in Figure 8.

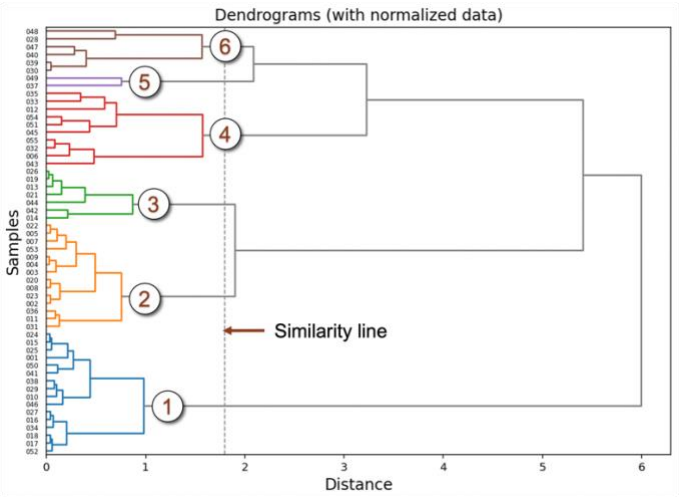

Figure 8: Dendrogram plot of hierarchical cluster analysis based on Euclidean distance for the Portola Valley dataset.

Multivariate PCA indicates that three principal components comprise 91.4% of the total variance in the dataset. Plotting the clusters in PC space, we can see a clear separation of clusters in the cross plot of the 2nd PC vs. the 3rd PC (Figure 9 right). Cluster 1 is rich in carbon dioxide; clusters 4, and 6 are rich in hydrogen; and cluster 6 is also rich in methane. Two samples that belong to cluster 5 exhibit anomalously high methane and ethane concentrations. This could be attributed to a nearby gas pipeline, an error in measurement, or a very localized phenomenon. Cluster 4 plots

on the North American Plate along the San Andreas Fault, and Cluster 1 plots in the northern regions where the fault zones become narrower.

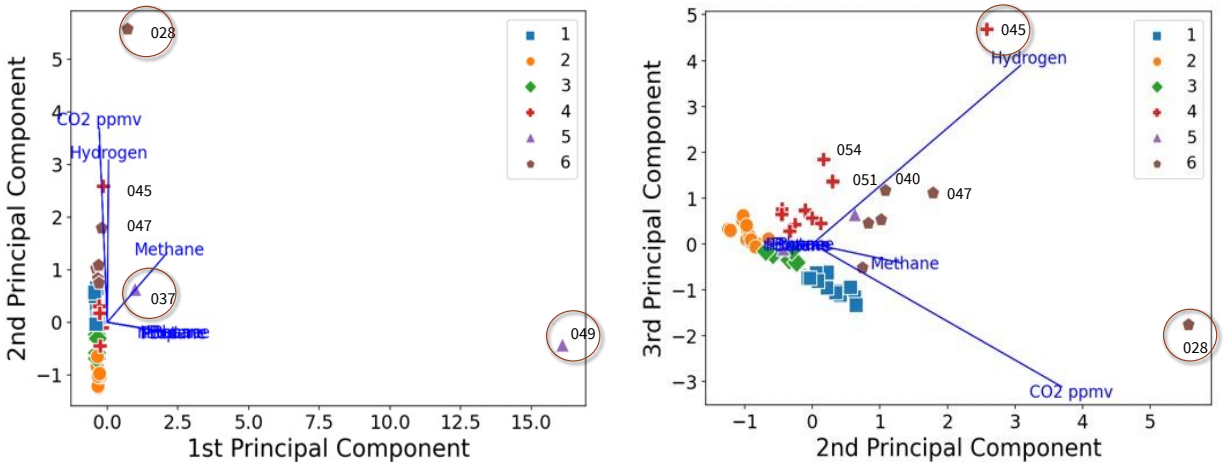

Figure 9: Portola Valley: Principal component plots show different clusters obtained through HCA, with odd samples highlighted. The lines are the loadings, highlighting the correlation of the clusters with the specific gas concentrations.

At Portola Valley, ALS indicates three endmembers for the gases including some samples with high methane and ethane concentrations (samples 49 and 37), which might be spurious. In Figure 10, there is linear mixing between the CO_2 endmember (Cluster 1) and hydrogen rich endmember (Cluster 4) with two samples plotting away from the linear mixing line. In Portola Valley, the highest concentrations of hydrogen are in the northern region in a zone of multiple faults (Figure 2c).

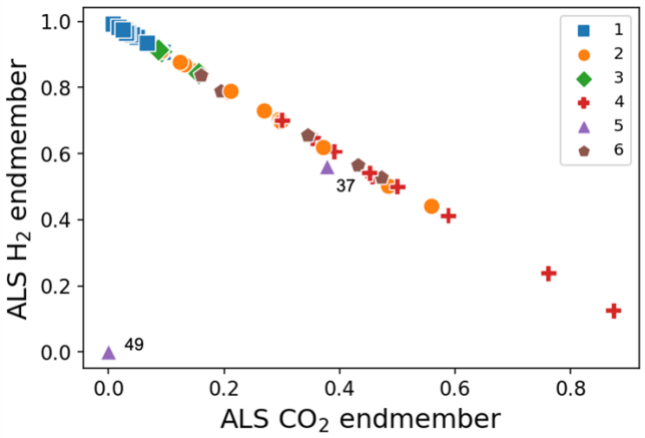

Figure 10: Component 1 vs. component 2 generated using alternating least squares regression for Portola Valley

4. Discussion

In both Jasper Ridge and Portola Valley, HCA and PCA identified separate clusters with high concentrations of carbon dioxide, hydrogen, and light hydrocarbons. Analysis using ALS established three gas endmembers in both study areas. The high concentrations of carbon dioxide are likely due to the aerobic degradation of organic matter by microbes to produce CO_2 as per the equation below:

$$C_6H_{12}O_6 + 6O_2 \rightarrow 6CO_2 + 6H_2O$$

The hydrocarbons are thermogenic and originated from the thermal degradation of organic matter. Hydrogen concentrations of up to ~30 times the background level were discovered. Finally, there is evidence that hydrogen originated due to faulting, serpentinization, or both, although deep-seated hydrogen seeping through the faults cannot be ruled out. Two spurious samples with high methane and ethane in Portola Valley were attributed to a localized source such as a nearby gas pipeline.

Generally, soils are net hydrogen sinks where hydrogen generated by microbial processes is immediately consumed as an energy source. H_2-producing and consuming microorganisms in the soil work in consortia, where generated hydrogen is immediately consumed by methanogenesis (Conrad, 1999), which consequently keeps the hydrogen concentrations low in the soil. Prinzhofer et al. (2019) reported 30 liters/week consumption of hydrogen from 1-m^3 of soil, which decreases measured hydrogen in the soil. Soil microbial activity to produce hydrogen has been studied mostly in the range of 0–30 cm but also at depths of up to two meters (Conrad, 1996). This activity also produces carbon dioxide and methane, and the soil is depleted of oxygen. In our observations in JRBP, the maximum concentration of carbon dioxide occurs in the southwest region of JRBP, whereas high H_2 concentrations occur near faults. Although we cannot eliminate minor contributions of microbial H_2, elevated contributions of hydrogen likely result from faults, serpentinization, and related geochemical processes. The amount of hydrogen could be much higher than those reported in the gas chromatography measurements due to dilution by air, as observed by Larin et al. (2015) while comparing measurements with portable handheld detectors and gas chromatography.

The presence of hydrocarbons in gas samples can be attributed to two processes that break down organic matter: thermal degradation, which generates thermogenic gas, and biodegradation, which produces microbial gas. Microbial gas is composed mainly of CH_4, with a $CH_4/(C_2H_6 + C_3H_8)$ ratio

greater than 100. Conversely, thermogenic gas contains more heavy hydrocarbons, resulting in $CH_4/(C_2H_6 + C_3H_8)$ ratios less than 100. In both study areas, the ratio was less than 100, with an average ratio of 29.41 in Portola Valley and 22.81 in Jasper Ridge. Thus, the origin of light hydrocarbons is dominantly thermogenic rather than microbial. The elevated H_2 concentrations can be either due to serpentinization or faulting. Multiple sources of fault-related hydrogen were proposed by Ware et al. (1984). The first process is purely mechanical and involves the crushing of rocks by the movement of a fault, which releases occluded hydrogen. The second method is chemical and involves freshly exposed rock surfaces that react with or catalyze the dissociation of groundwater. The third method combines chemical reactions of water with FeO in rocks and magmas with mechanical fracturing of rocks by fault movement to release hydrogen. Finally, a fourth process involves a deep source in the mantle that produces both hydrogen and methane. More investigations to determine stable carbon isotopic composition need to be done to establish the sources with greater certainty.

Time sequence analysis in both regions shows an initial increase due to perturbation in the soil gases and subsequent release of adsorbed gases in the soil that finally equilibrates after ~24 hours. With limited data on repeatability at different sampling locations, it is difficult to comment on the diurnal variations in the gases. Fluctuations in the concentrations of gases in the soil are also influenced by various environmental factors, such as changes in the temperature of the air and soil, pressure, soil moisture, and wind. These factors are generally associated with changes in the amount of solar radiation received by the soil and are not considered in this study.

Soil gas sampling is a cost-effective and preliminary way to explore natural hydrogen. Osselin et al. (2022) discussed stimulating the production of hydrogen in regions that possess suitable rocks and have the propensity to generate hydrogen. The presence of hydrogen confirmed through geochemical soil sampling and data analysis in different regions can also be coupled with stimulation of reactions such as serpentinization to produce hydrogen at the required rates.

5. Conclusions

Extensive sampling was carried out in the Jasper Ridge Biological Preserve and Portola Valley regions near the San Andreas Fault to study the generation of hydrogen through serpentinization and faulting. Multivariate statistical analysis of the gas concentration dataset was carried out, including hierarchical cluster analysis, principal component analysis, and alternating least squares

regression to differentiate different clusters and study spatial variability. After analyzing the dataset, the following conclusions were drawn:

- Elevated concentrations (~30-35 times background level) of hydrogen occur in both study areas, up to 20.32 ppmv in Jasper Ridge and 17.3 ppmv in Portola Valley.
- Most samples with high hydrogen values fall on or near faults with higher concentrations in Jasper Ridge, where we observed exposures of serpentinite.
- High carbon dioxide concentrations in samples at low elevations near the water table result from the aerobic degradation of organic matter by microbes to produce CO_2.
- The concentrations of light hydrocarbons are due to the thermal cracking of organic matter.
- Time sequence analysis shows the effect of initial perturbation in the soil gas samples and eventual equilibration after about ~24 hours.
- Geochemical soil gas sampling followed by rigorous data analysis can be a low-cost preliminary exploration tool for natural as well as stimulated hydrogen exploration.

Acknowledgments

We thank Nona Chiariello and Bill Gomez, staff members of Jasper Ridge Biological Preserve, for facilitating our fieldwork there. We thank Stephan Graham, former Dean of the erstwhile Stanford School of Earth, Energy and Environmental Sciences, for helping to plan the fieldwork and getting the requisite permissions, and for providing funding. We acknowledge funding from the sponsors of Stanford's Natural Gas Initiative (NGI), Stanford Center for Earth Resources Forecasting (SCERF) and Basin Processes and Subsurface Modeling (BPSM) programs. We also acknowledge Dalton Balentine, staff member of Geofrontiers, for accompanying us during the fieldwork and Gary Rice for his assistance. Further, we thank Howard Young, town manager of Portola Valley, for his assistance and permission to sample at Portola Valley. Chester Wrucke and Robert Wrucke helped with reconnaissance surveys and fault identification in Portola Valley.

References

Arai, T., Okusawa, T., & Tsukahara, H. (2008). Behavior of gases in the Nojima fault zone revealed from the chemical composition and carbon isotope ratio of gases extracted from DPRI 1800 m drill core. *Island Arc*, *10*(3–4), 430–438. https://doi.org/10.1111/j.1440-1738.2001.00341.x

Boreham, C. J., Sohn, J. H., Cox, N., Williams, J., Hong, Z., & Kendrick, M. A. (2021). Hydrogen and hydrocarbons associated with the Neoarchean Frog's Leg Gold Camp, Yilgarn Craton, Western Australia. *Chemical Geology*, *575*, 120098. https://doi.org/10.1016/j.chemgeo.2021.120098

Coleman, R. G. (2004). Geologic nature of the Jasper Ridge Biological Preserve, San Francisco Peninsula, California. *International Geology Review*, *46*(7), 629-637.

Conrad, R. (1996). Soil microorganisms as controllers of atmospheric trace gases (H2, CO, CH4, OCS, N2O, and NO). *Microbiological reviews*, *60*(4), 609-640.

Conrad, R. (1999). Contribution of hydrogen to methane production and control of hydrogen concentrations in methanogenic soils and sediments. *FEMS microbiology Ecology*, *28*(3), 193-202.

Coveney Jr, R. M., Goebel, E. D., Zeller, E. J., Dreschhoff, G. A., & Angino, E. E. (1987). Serpentinization and the origin of hydrogen gas in Kansas. *AAPG Bulletin*, *71*(1), 39-48. https://doi.org/10.1306/94886D3F-1704-11D7-8645000102C1865D

Deville, E., & Prinzhofer, A. (2016). The origin of N2-H2-CH4-rich natural gas seepages in ophiolitic context: a major and noble gases study of fluid seepages in New Caledonia. *Chemical Geology*, *440*, 139-147. https://doi.org/10.1016/J.CHEMGEO.2016.06.011

Fong-liang, J., & Gui-ru, L. (1981). The application of geochemical methods in earthquake prediction in China. *Geophysical Research Letters*, *8*(5), 469-472.

Gaucher, E. C. (2020). New perspectives in the industrial exploration for native hydrogen. *Elements: An International Magazine of Mineralogy, Geochemistry, and Petrology*, *16*(1), 8-9.

Gunes, B. (2021). A critical review on biofilm-based reactor systems for enhanced syngas fermentation processes. *Renewable and Sustainable Energy Reviews*, *143*, 110950.

Han, J., Liang, Y., Hu, J., Qin, L., Street, J., Lu, Y., & Yu, F. (2017). Modeling downdraft biomass gasification process by restricting chemical reaction equilibrium with Aspen Plus. *Energy conversion and management*, *153*, 641-648.

Hao, Y., Pang, Z., Tian, J., Wang, Y., Li, Z., Li, L., & Xing, L. (2020). Origin and evolution of hydrogen-rich gas discharges from a hot spring in the eastern coastal area of China. *Chemical Geology*, *538*, 119477. https://doi.org/10.1016/J.CHEMGEO.2020.119477

Hastie, T., Tibshirani, R., and Friedman, J., 2001, The elements of statistical learning: Data mining, inference, and prediction, Springer-Verlag, NY., 533pp.

IEA (2021), Net Zero by 2050, IEA, Paris https://www.iea.org/reports/net-zero-by-2050, License: CC BY 4.0

Isaev, E. I., Skorodumova, N. V., Ahuja, R., Vekilov, Y. K., & Johansson, B. (2007). Dynamical stability of Fe-H in the Earth's mantle and core regions. *Proceedings of the National Academy of Sciences*, *104*(22), 9168-9171. https://doi.org/10.1073/pnas.0609701104.

Jalalvand, A. R., & Goicoechea, H. C. (2017). Applications of electrochemical data analysis by multivariate curve resolution-alternating least squares. *TrAC Trends in Analytical Chemistry*, *88*, 134-166.

Jasper Ridge Biological Preserve (Agency). (2017). Geologic Fault Lines, Jasper Ridge Biological Preserve, 1997. [Shapefile]. Jasper Ridge Biological Preserve (Agency). Retrieved from https://earthworks.stanford.edu/catalog/stanford-rg697hg6565.

Jones, V. T., & Pirkle, R. J. (1981, March). Helium and hydrogen soil gas anomalies associated with deep or active faults. In *Proc. of the 1981 American Chemical Society Annual Meeting, Atlanta, GA* (pp. 17666-17672).

Kita, I., Matsuo, S., & Wakita, H. (1982). H_2 generation by reaction between H_2O and crushed rock: an experimental study on H_2 degassing from the active fault zone. *Journal of Geophysical Research: Solid Earth*, *87*(B13), 10789-10795.

Larin, V. N. (1993). Hydridic earth: the new geology of our primordial hydrogen-rich planet, Polar Pub.

Larin, N., Zgonnik, V., Rodina, S., Deville, E., Prinzhofer, A., & Larin, V. N. (2015). Natural molecular hydrogen seepage associated with surficial, rounded depressions on the European craton in Russia. *Natural Resources Research*, *24*, 369-383. https://doi.org/10.1007/s11053-014-9257-5

Lyndgaard, L. B., van den Berg, F., & de Juan, A. (2013). Quantification of paracetamol through tablet blister packages by Raman spectroscopy and multivariate curve resolution-alternating least squares. *Chemometrics and Intelligent Laboratory Systems*, *125*, 58-66.

Murray, A. P., & Peters, K. E. (2021). Quantifying multiple source rock contributions to petroleum fluids: Bias in using compound ratios and neglecting the gas fraction. *AAPG Bulletin*, *105*(8), 1661-1678.

Neal, C., & Stanger, G. (1983). Hydrogen generation from mantle source rocks in Oman. *Earth and Planetary Science Letters*, *66*(C), 315–320. https://doi.org/10.1016/0012-821X(83)90144-9

Nivin, V. A., Pukha, V. V., Lovchikov, A. V., & Rakhimov, R. G. (2016, December). Changes in the molecular hydrogen concentration in an underground mine (Lovozero rare-metal deposit, Kola peninsula). In *Doklady Earth Sciences* (Vol. 471, pp. 1261-1264). Pleiades Publishing. https://doi.org/10.1134/S1028334X16120060

Oey, M., Sawyer, A. L., Ross, I. L., & Hankamer, B. (2016). Challenges and opportunities for hydrogen production from microalgae. *Plant biotechnology journal*, *14*(7), 1487-1499.

Osselin, F., Soulaine, C., Fauguerolles, C., Gaucher, E. C., Scaillet, B., & Pichavant, M. (2022). Orange hydrogen is the new green. *Nature Geoscience*, *15*(10), 765-769. https://doi.org/10.1038/s41561-022-01043-9

Prinzhofer, A., Tahara Cissé, C. S., & Diallo, A. B. (2018). Discovery of a large accumulation of natural hydrogen in Bourakebougou (Mali). *International Journal of Hydrogen Energy*, *43*(42), 19315–19326. https://doi.org/10.1016/j.ijhydene.2018.08.193

Prinzhofer, A., Moretti, I., Françolin, J., Pacheco, C., D'Agostino, A., Werly, J., & Rupin, F. (2019). Natural hydrogen continuous emission from sedimentary basins: The example of a Brazilian H_2-emitting structure. *International Journal of Hydrogen Energy*, *44*(12), 5676–5685. https://doi.org/10.1016/J.IJHYDENE.2019.01.119

Redwood, M. D., Orozco, R. L., Majewski, A. J., & Macaskie, L. E. (2012). An integrated biohydrogen refinery: synergy of photofermentation, extractive fermentation and hydrothermal hydrolysis of food wastes. *Bioresource technology*, *119*, 384-392.

Rogozhin, E. A., Gorbatikov, A. V., Larin, N. V., & Stepanova, M. Y. (2010). Deep structure of the Moscow Aulacogene in the western part of Moscow. *Izvestiya. Atmospheric and Oceanic Physics*, *46*(8), 973.

Satake, H., Ohashi, M., & Hayashi, Y. (1984). Discharge of H 2 from the Atotsugawa and Ushikubi Faults, Japan, and its relation to earthquakes. *Pure and Applied Geophysics*, *122*, 185-193. https://doi.org/10.1007/BF00874592

Sato, M., Sutton, A. J., & McGee, K. A. (1984). Anomalous hydrogen emissions from the San Andreas fault observed at the Cienega Winery, central California. *Pure and Applied Geophysics*, *122*, 376-391. https://doi.org/10.1007/BF00874606

Sato, M., Sutton, A. J., McGee, K. A., & Russell-Robinson, S. (1986). Monitoring of hydrogen along the San Andreas and Calaveras faults in central California in 1980-1984. *Journal of Geophysical Research: Solid Earth*, *91*(B12), 12315–12326. https://doi.org/10.1029/jb091ib12p12315

Shcherbakov, A. V., & Kozlova, N. D. (1986). Occurrence of hydrogen in subsurface fluids and the relationship of anomalous concentrations to deep faults in the USSR. *Geotectonics*, *20*, *120-128*.

Shirokov, V. A., Firstov, P. P., Makarov, E. O., Stepanov, I. I., & Stepanov, V. I. (2015). An Approach to the short- and long-term forecasting of strong earthquakes: A case study of the M w = 9.0 Tohoku earthquake, Japan, March 11, 2011. *Seismic Instruments*, *51*(3), 229–241. https://doi.org/10.3103/s074792391503010x

Sloan, D. (2006). *Geology of the San Francisco Bay Region* (No. 79). Univ of California Press.

Sugisaki, R., Ido, M., Takeda, H., Isobe, Y., Hayashi, Y., Nakamura, N., Satake, H., & Mizutani, Y. (1983). Origin of hydrogen and carbon dioxide in fault gases and its relation to fault activity. *The Journal of Geology*, *91*(3), 239-258.

Toulhoat, H., & Zgonnik, V. (2022). Chemical Differentiation of Planets: A Core Issue. *The Astrophysical Journal*, *924*(2), 83. https://doi.org/10.3847/1538-4357/ac300b

Wakita, H., Nakamura, Y., Kita, I., Fujii, N., & Notsu, K. (1980). Hydrogen release: New indicator of fault activity. *Science*, *210*(4466), 188–190. https://doi.org/10.1126/science.210.4466.188

Ware, R. H., Roecken, C., & Wyss, M. (1984). The detection and interpretation of hydrogen in fault gases. *Pure and Applied Geophysics PAGEOPH*, *122*(2–4), 392–402. https://doi.org/10.1007/BF00874607

Wiersberg, T., & Erzinger, J. (2008). Origin and spatial distribution of gas at seismogenic depths of the San Andreas Fault from drill-mud gas analysis. *Applied Geochemistry*, *23*(6), 1675-1690

Zgonnik, V. (2020). The occurrence and geoscience of natural hydrogen: A comprehensive review. *Earth-Science Reviews*, *203*, 103140.